

Efficiency Focused Energy Management Strategy Based on Optimal Droop Gain Design for More Electric Aircraft

Mohamed A. A. Mohamed, *Student Member, IEEE*, Seang Shen Yeoh, Jason Atkin, Habibu Hussaini, and Serhiy Bozhko, *Senior Member, IEEE*

Abstract—Due to the substantial increase of the number of electrically-driven systems on-board More Electric Aircraft (MEA), the on-board Electric Power Systems (EPS) are becoming more and more complex. Therefore, there is a need to develop a control strategy to manage the overall EPS energy flow and ensure the operation of safety-critical systems (which are electrical loads) under different operating scenarios, and to consider EPS losses minimization, exploiting the thermal capability of generators, different load priorities, as well as available batteries with their charging and discharging schedules. This paper presents an Energy Management (EM) strategy that considers the aforementioned objectives. The optimal droop gain approach is employed as a power-sharing method to minimize the total EPS losses in MEA. A Finite State Machine (FSM) has been used to implement the control strategy to realize the EPS re-configuration operation. The proposed EM strategy is implemented and simulated using Matlab/Simulink and Hardware In the Loop (HIL) under the different operational scenarios such as normal operations, failure of one of the power generation channels, and failure of all power generation channels. The proposed EM method has shown its capability to efficiently manage the EPS under different operating conditions to reduce the overall system losses.

Index Terms—Energy Management, DCMG, MEA, Droop Gains

I. INTRODUCTION

MORE Electric Aircraft (MEA) technology aims to increase the use of electrical power to reduce the use of non-propulsive power source, e.g. pneumatic, mechanical, and hydraulic [1]–[3]. This would bring in significant changes in the electric power system in terms of power generation, transmission, and distribution[4]–[7]. The four typical EPS architectures for MEA are constant frequency AC EPS, hybrid AC, and DC EPS, hybrid High Voltage (HV) AC, and

This work was supported by the Egyptian Government ministry of higher education (cultural affairs and missions sector) and the British Council through Newton-Mosharafa fund. The authors also gratefully acknowledge support from the ESTEEM project which received funding from the Clean Sky 2 Joint Undertaking under the European Union’s Horizon 2020 research and innovation programme under grant agreement No 755485. (Corresponding author: Mohamed A. A. Mohamed). Mohamed A. A. Mohamed is with the Power Electronics, Machines, and Control Group (PEMC), University of Nottingham, Nottingham NG7 2RD, U.K., and also with the electrical engineering department, Assiut University, Assiut, Egypt, 71515 (e-mail: mohamed_elbesealy@eng.au.edu.eg, Mohamed.Mohamed1@nottingham.ac.uk). Seang Shen Yeoh, Jason Atkin, Habibu Hussaini, and Serhiy Bozhko are with the Power Electronics, Machines, and Control Group (PEMC), University of Nottingham, Nottingham NG7 2RD, U.K. (e-mail: seang.yeoh@nottingham.ac.uk, jason.atkin@nottingham.ac.uk, ezhh3@nottingham.ac.uk, serhiy.bozhko@nottingham.ac.uk)

HVDC EPS, and pure HVDC EPS [8]. Pure HVDC topology mainly distributes power in DC form, and it is considered a very promising architecture for future MEAs [9], [10]. As the demand of electric power on-board modern aircraft rises dramatically, the low maintenance and high EPS reliability are essential for the design of future MEA. The 270 HVDC EPS concept is now considered as optimal option for future aircraft due to its relative simplicity, flexibility, and unique ability of DC systems to supply uninterrupted power to electrical loads[11], [12]. One of possible HVDC EPS architecture is shown in Fig. 1, the generators with corresponding Active Front-End (AFE) converters and batteries with corresponding bidirectional DC/DC converters are connected to the 270 HVDC bus by solid-state power controllers (SPPC) C1-C3 and C10-C11. These types of switches are used for communication of the EPS, as well as to control the power flow and to reconfigure the topology of the EPS by creating new connections between EPS elements. Different system reconfigurations can be obtained by changing the status of the circuit

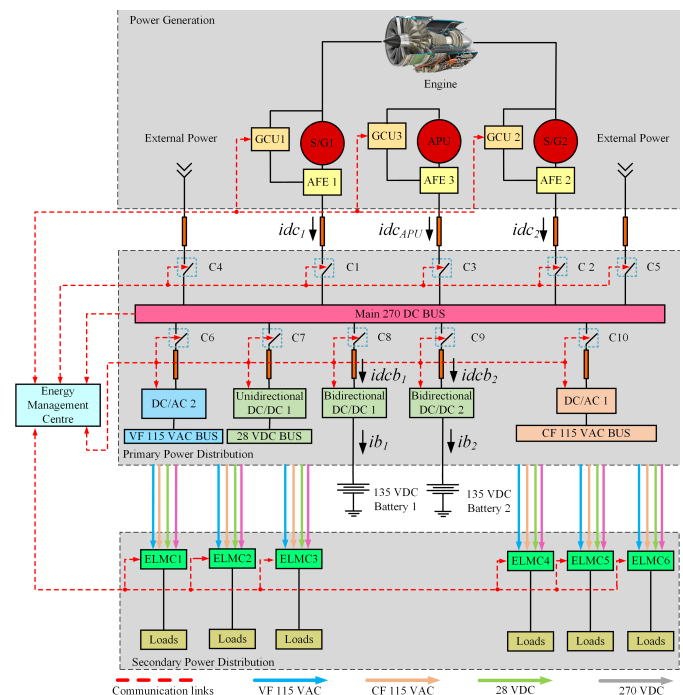


Fig. 1. Promising MEA EPS architecture

breakers (open/closed). For example, when one of the power generation channels fails, the Auxiliary Power Unit (APU) or battery system may be used to supply some emergency buses to enable safety-critical operations. The energy Management strategy is required to manage the power flow distribution and EPS reconfigurations, setting a new power path and ensuring safe operation under different operating scenarios. The power distribution is a remote distribution as shown in Fig. 2 which means the power generated and distributed efficiently near to its consumptions and is divided into three stages i.e. power generation, primary power distribution, and secondary power distribution. At the power generation level, there are two main Permanent Magnet Machines (PMM) driven by one engine that works as Starter/Generator (S/G) and one APU, all interfaced with 270 V single DC bus through AFE converters. The APU is used as a backup power source during flight and provides power to the power users during ground operations, which makes the airplane electrically self-sufficient on the ground. The AFE converter controls the speed and the DC bus voltage of the S/G PMM during starting and generating modes respectively, besides other functions i.e. overvoltage protection, parallel generator operation and others. There are four different voltage buses at the primary power distribution stage to supply different loads types, namely: Variable Frequency 115/ VAC, constant frequency 115 VAC/400 Hz, and 28 VDC, beside 270 HVDC. The conversion to different operating voltages to drive all of the onboard loads types is performed using the power converters. The authors in this study used the available loads analysis data for the Flying Crane aircraft. Flying Crane is a medium to short haul aircraft with 130 seats which is mainly aimed at the Chinese domestic air transport market. Also, it is considered to be a competitor of those current B737 series and A320 series aircraft [12]. The secondary power distribution system includes six Electric Load Management

Centres (ELMC) to deliver and manage power to the loads as shown in Fig. 2. In terms of emergencies, the EPS relies on power from two Li-ion batteries. these batteries are used to provide emergency power for the high priority loads, when faults occur in a flight, and for starting the APU. The Li-ion is chosen because it has the right functionality and chemistry to deliver a large amount of power in a short time. HV distribution is recommended to reduce the size of conductors and power losses of the system. To realize a stable and reliable flight mission and improve the energy efficiency of MEA, an EM strategy is used.

A. Typical Implementation of Energy Management

In today's aircraft Electric Load Management (ELM) based on fixed priorities of loads is often implemented [13]. The loads can be shed and reconnected depending on their importance during the flight. There is often a fixed, predefined priority for each controllable load and the higher priority load will be shed later. The power of the generators and the loads are measured to determine the number of loads to be shed. Often a set of similar loads are connected to one switch [13]. In case of many loads with the same priority, the ELM uses by additional criteria to determine which loads are shed and which are not. One solution is to shed the large loads first, this keeps as many loads as possible connected. Another solution is to find a set of loads which consume as much as possible of generator capacity and this called "Knapsack problem" [13]. The advantages of ELM strategy are a simple basic implementation, just defining the priorities for each load and thresholds at which shedding and reconnection take place, and that proven and mature algorithms are available for it since, it has been applied for decades. Regarding the disadvantages, ELM is limited to switchable loads in most cases and cannot deal sufficiently with continuously controllable loads. The priorities of loads is may not fixed during flight, these can depends on the flight phase and other conditions and this is not consider by the typical ELM. Further, ELM is not capable of optimizing the system efficiency or reducing the size and weight of EPS.

B. Energy Management Strategy

The goal of an EM strategy is to ensure the stability and quality of the EPS network by managing power flow while respecting nominal operating points and avoiding unfavourable conditions of usage i.e. high cycling rates for batteries or high dynamics power demands for generators [14]. Moreover, during the development of EPS EM strategies, the safe operation of the EPS is another critical factor to consider. By designing the right EM strategy: the system weight is minimised hence, the overall efficiency is improved. Further, a properly designed management strategy provides the potential for the aircraft to operate at its maximum performance under fault conditions. To achieve these aims the controller can be given the task of reconfiguring the system by switching on or off a number of circuit breakers based on the reconfiguration strategy [15]. The reconfiguration approach is utilized to find the correct power path for each load to be fed by using

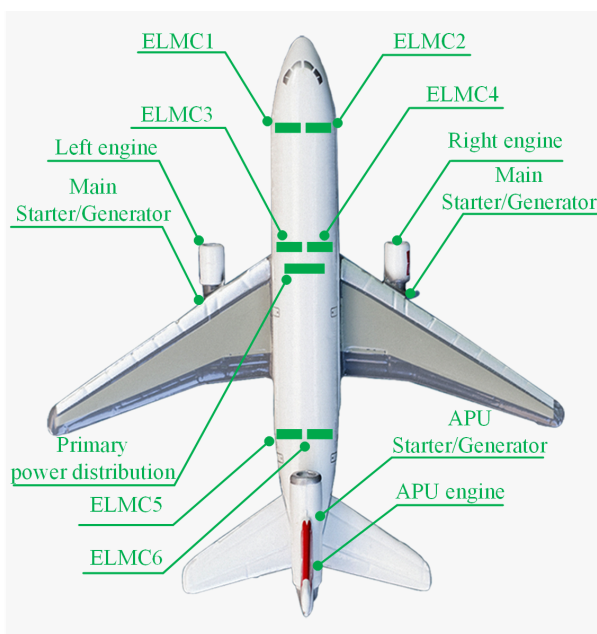


Fig. 2. Layout of power distribution system [12]

switches while considering the optimization of the system in terms of power flow and avoiding unsafe configurations [16], [17]. The EPS is managed by the control system in order to maintain an uninterruptible power supply for loads. However, rules must be defined to avoid unsafe conditions such as creating parallel power paths between two sources or discharging of the batteries beyond a pre-set limit.

In [15] a control strategy to manage the power flow in the EPS and ensure continuous power supply to the high priority loads under different power converter failures for MEA is presented. The proposed strategy is applied through a smart controller and the control logic is implemented using the FSM approach. The actions taken by the controller under different operating conditions are dependent on the state of charge of the batteries. In [18] the balance between the aircraft power supply (gas turbine generator and storage device) and power demands, while minimizing the operation cost including fuel and battery operation cost, is formulated as Mixed-Integer Non-linear Programming (MINLP) power management problem for MEA civil aircraft. The outputs of MINLP are the optimal active power generation, load management, and battery charging/discharging status. In [19] a power allocation and load management method to minimize the load shedding is presented. The management problem is formulated as Mixed-Integer Quadratic Problem (MIQP) where the decision variables are the generator output power, load connections, and battery charging schedules.

The controller which performs different functions of EM strategy such as provide uninterruptible power, ensure safe operation of the EPS, etc can be implemented using different methods e.g. FSM. FSM method is a way of formalizing the logic of a controller, where the controller is considered to be in one of a set number of states, and will transition to other states (or the same state) during its operation, potentially setting some outputs as a consequence of the state it is in or the transitions it performs. When Linear Temporal Logic (LTL) is used to specify a controller, a ‘controller synthesis’ step is usually performed, whereby an FSM is automatically generated from the LTL formulation. However, it is still much more common the generate an FSM manually and has for many years been considered a suitable tool for the control logic design of EPS management, as well as being applied to model problems in many other areas, including mathematics and artificial intelligence. FSM is a computation model that can be used to simulate sequential logic and can be implemented with hardware or software. In FSM, it is possible to model the behaviour of the system as a set of states and transitions between states, which are known as reactive systems [20]. The advantages of using FSM for controller design are that it is easy to use and visualize, and formulations already exist for many powerful and fast algorithms [15].

To the best of the author’s knowledge, there is a lack in the research conducted in the area of proposing an intelligent energy management strategy to ensure uninterruptible power supply to safety-critical loads and considering system losses minimization (converters and transmission lines losses), exploiting the thermal capability (overload) of generators, considering variable load priority during flight phases and schedules of

batteries charging/discharging, to supplying safety-critical and non-critical loads during different failure scenarios. The main contributions of this paper can be summarized as follows:

- Proposing a smart EM strategy that ensures the safety-critical loads are powered under different flight scenarios by reconfiguring the EPS. Furthermore, the proposed EM considers the exploitation of generators thermal capability, variable load priority, system losses minimization, and battery charging/discharging schedules.
- Utilising the FSM approach to implement the proposed EM strategy logic in the controller as it is easy to use, visualize, and contains fast and powerful algorithms.

The rest of the paper is divided into 4 sections as follows: Section II presents the load analysis required for system components sizing and loads priority setting. Section III shows the proposed EM strategy and state transition between different operating scenarios and corresponding system switches and variables setting. Section IV shows the validation of the proposed method. Finally, Section VII presents the conclusion.

II. LOAD ANALYSIS

The first step of EPS design is understand the electric load requirement as the EPS aims to provide electric power to all of the onboard loads. Moreover, Load analysis is important to determine the required generating capacity and the required number of main power sources. It is recommended that the majority of loads should be the same voltage type as the primary source. The authors in this study have used the available report on load analysis for the Flying Crane aircraft [12]. The load analysis must include continuous analysis, 5-minute analysis and 5-second analysis. Due to the confidentiality issues, the detailed load information cannot be obtained, therefore, the 5-second analysis cannot be including in this study [12]. All of these loads are divided into different categories based on their functions as follows:

- Low Priority Loads (LPL): these are not related to flight safety and can be shed in case of power generation shortage.
- Medium Priority Loads (MPL): these loads are required to operate aircraft safely. Some of them can be shed in case of deficiency of generated power, for example when only one generator is operating.
- High/critical Priority Loads (HPL): these loads are critical for the flight safety, hence must operate under any circumstance during flight, even after in the harshest emergency situation.

Table I shows the load analysis results for Flying Crane aircraft including continuous (C) and Intermittent (T) or 5-minute loads and divided into LPLs, MPLs, and HPLs. The total continues loads during each flight phase is given with and without the intermittent loads. It should be noted that the Environmental Control System (ECS) power requirement takes nearly half of the total power required and ECS is powered by 270 VDC. The obtained load analysis data mentioned above is used as a case study to verify the proposed EM strategy. In the next section, the proposed EM strategy is discussed in detail.

TABLE I
FLYING CRANE AIRCRAFT DATA

| Load category | Ground | Take-off | Climb | Cruise | Descending | Loiter | Landing | Unit |
|-------------------------------|--------|----------|--------|--------|------------|--------|---------|---------|
| LPLs (Include C) | 8.25 | 7.4 | 39.68 | 50.3 | 39.68 | 7.4 | 40.53 | kW |
| LPLs (Include C and T) | 10.25 | 7.4 | 39.68 | 50.3 | 39.68 | 7.4 | 53.83 | kW |
| MPLs (Include C) | 281.2 | 327.73 | 328.53 | 291.82 | 328.53 | 315.8 | 315.73 | kW |
| MPLs (Include C and T) | 291.2 | 343.53 | 328.53 | 304.53 | 338.53 | 315.8 | 346.93 | kW |
| HPLs (Include C) | 4 | 3 | 3 | 3 | 3 | 3 | 3 | kW |
| Total loads (Include C) | 293.5 | 338.13 | 271.21 | 345.12 | 371.21 | 326.2 | 359.26 | kW |
| Total loads (Include C and T) | 305.5 | 353.93 | 371.21 | 357.83 | 381.21 | 326.2 | 403.75 | kW |
| Duration | t_1 | t_2 | t_3 | t_4 | t_5 | t_6 | t_7 | Seconds |

III. ENERGY MANAGEMENT STRATEGY

This section outlines the proposed control strategy: as mentioned above, this strategy aims to ensure uninterrupted power to the HPLs. Moreover, the batteries are employed to supply the medium priority loads during generator failures in addition to their basic functions such as providing power to start the APU and supporting ground operations (refuelling, powering the braking system when the airplane is towed, etc). Moreover, keeping the batteries State of Charge (SoC) within the pre-set values. The assumptions for EM strategy investigated in this study are:

- 1) Electrical loads can be either powered or shed (on/off). Loads can be regulated continuously or intermittently.
- 2) Generators can operate above their nominal power (10%) for a short time (5 minutes). This overload capacity can be exploited.
- 3) The EPS can be reconfigured, using switches, to find the appropriate power path for each load to be fed in different situations.
- 4) Storage devices can both absorb and supply the referenced power (when available).
- 5) The APU generator will come into an operation in case of the failure of the one of main generation. The APU generator can run in parallel with the remaining main generator.
- 6) APU generator is used to provides power to the power users during ground operation.

From the discussion in Section I-B it can be seen that the EPS is a reactive system, i.e. continuously having to react to external and internal stimuli. Therefore, based on [16], [21], the use of FSM is considered as a solution to improve EPS management. In FSM, the behaviour of the system can be modelled as a set of states and transitions between states. From a mathematical point of view, the FSM can be seen as:

$$f\left(\sum, S, s_0, \delta, F\right) \quad (1)$$

where \sum represents a finite set of symbols, S is a finite set of sates, s_0 is the initial state, so that $s_0 \in S$, δ is a state transition function.

$$\delta : S \times \sum \rightarrow S \quad (2)$$

Here, F is the finite set of final states. An example of the formulation is depicted in Fig. 3.

The following equations describe the system in Fig. 3. The inputs are:

$$\sum = [\varepsilon] \quad (3)$$

The states can be expressed as:

$$S = [s_0, s_1, s_2] \quad (4)$$

The transition function δ that define mapping between cartisian product of the set of states S and the language symbols \sum into the set of states S is given by:

$$\delta = [s_0/\varepsilon_{01} \rightarrow s_1, s_1/\varepsilon_{12} \rightarrow s_2, s_2/\varepsilon_{20} \rightarrow s_0] \quad (5)$$

For example, if the current state is s_0 and the input is ε_{01} , the next state will be s_1 and so on. The final state can be given as:

$$F = s_2 \quad (6)$$

Since the theory of FSM has been introduced, it can be applied to the EPS in order to set a management strategy. The operating modes can be divided into 5 main scenarios and 12 sub scenarios based on the status of electric power system components and these modes are explained as follows:

A. Normal scenario

- **State 1 (ST1): No fault of main generators, all loads connected and supplied, and APU off**

In this state, there is no fault in the power generation channels and the Energy Management Centre (EMC) role is to send a message to ELMC to connect the loads according to each flight phase. If the EPS was operating in a different scenario and transition to ST1 happened then, the EMC should shut down the APU if it is running, unshed the loads if they were shed, and charge the batteries if their $(SoC) < SoC_{max}$.

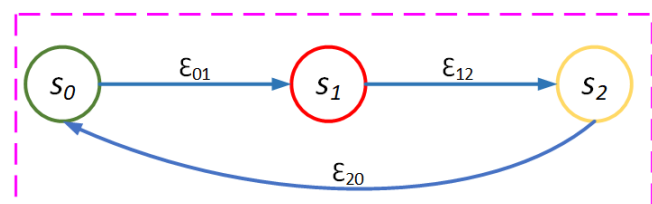


Fig. 3. Example of reactive system

B. Both Power Generation Channels Fail and APU is Started Scenario

- **State 2 (ST2): Main generators failed and APU running for up to 5 minutes**

In this state, both main power generation channels failed and APU is running. The APU can be overloaded by 10% for 5 minutes and batteries can be used until discharging to the lower limit SoC_{min} .

- **State 3 (ST3): Main generators failed, APU overloaded for more than 5 minutes, batteries discharging, and low priority loads shed**

Here, the APU overloading in ST2 has occurred for more than 5 minutes, but the batteries still have enough energy to supply the loads. Therefore, the batteries continue to supply power (discharge further), however the low priority loads are shed.

- **State 4 (ST4): Main generators failed, APU overloaded more than 5 minutes, batteries permitted to charge, and all LPLs and some MPLs shed**

This state reached from ST3 if the batteries were discharging and reached the lower limit SoC_{min} , so that they could no longer provide power, and the APU can still provide its rated power (250 kW). The LPLs, MPL1 and MPL2 loads are all shed in this state to reduce the power requirements. If there is surplus power after shedding, the batteries can be charging.

- **State 5 (ST5): Main generators failed, APU overloaded less than 5 minutes, batteries charging and LPLs and some MPLs shed**

If the overloading time does not reach 5 minutes and the batteries are discharging, then the EMC allows the APU to run with 10% overloading condition. The LPLs, MPL1, and MPL2 are all shed in this state, to reduce the power requirements. If there is a surplus power after shedding, the batteries can be charging.

C. One Power Generation Channels Fails and APU Fails Scenario

- **State 6 (ST6): One generator running with 10% overload up to 5 minutes and batteries discharging**

Only one of the main generators is working, and it is allowed to be overloaded by 10 % for 5 minutes with batteries discharging at their maximum rates to cover the shortage in power demand.

- **State 7 (ST7): One generator running, batteries discharging ($SoC \geq SoC_{min}$), healthy generator is overloaded for more than 5 minutes, batteries discharged, and LPLs shed**

Once the overloading time of the healthy generator reaches 5 minutes and the SoC of the batteries is above their minimum values, the operating point will move to ST8, in which case the batteries will discharge until their minimum SoC values and LPLs are shed.

- **State 8 (ST8): One generator running, no overload, batteries charging ($SoC \leq SoC_{min}$), LPLs and some MPLs shed**

In this operating state, the batteries are fully discharging and the available generating power is equal to 250 kW. Therefore, the LPLs, MPL1, and MPL2 are shed and the batteries will charge until their maximum values.

- **State 9 (ST9): One generator running in overload (5 minutes), batteries charging, LPLs and MPLs shed**

If the overloading time is not reached the limit (5 minutes) and the batteries have been discharging below SoC_{min} , then the system is in ST9. The healthy generator is overloaded by 10%. The LPLs, MPL1, and MPL2 are all shed in this state, to reduce the power requirements. If there is a surplus power after shedding, the batteries can be charging.

D. One of Power Generation Channels is Failed and APU is Started Scenario

- **State 10 (ST10). One generator and APU running and not overloaded, batteries charging, loads unshed**

In this state, the APU has started, it is similar to the normal scenario (ST1). Therefore, the loads which were shed in previous scenario get unshed and the EMC will not allow the healthy generator to be overloaded more, and the batteries will charge until SoC_{max} .

E. Both Main Power Generation Channels Fail and APU Fails/Not started Scenario (Emergency)

- **State 11 (ST11): Main generators and APU fail and SoC less than SoC_{min}**

In this state, all power sources except batteries have failed, and the batteries supply the critical loads only to allow the aircraft landed safely.

- **State 12 (ST12): Main generators and APU fail and SoC greater than SoC_{min}**

If there is enough power in the batteries, this can be exploited by supplying MPL1 and/ MPL2.

Fig. 4 illustrates all the states with simplified and reduced scale EPS diagram. The failed elements are marked with red crosses. Fig. 5 shows the EM strategy adopted in this work, the EM strategy covers all operation modes which includes normal, failure of one power generation channels, failure of both power generation channels, and emergencies case. Moreover, the conditions for transitions between states are explained in the next section.

As is clear in the figure, there is a reciprocal transition between the major scenarios, and the directions of the arrows illustrate this. The transition will occur between the main scenario firstly, and subsequently between the inside states. For example, if the system is operating in the normal scenario and both main generators fail, the EM system will switch to the emergency scenario. There are two states in the emergency scenario, ST11, and ST12, which are selected dependent on the SoC of the batteries. The same goes for the other direction. The EM system will return to normal operation once the fault has been cleared. However, if one of the main generators fails and the other remains faulty, the EM system will switch to the “one of the main generators failure scenario,” and the EM system will start at ST6 and move from and to any state

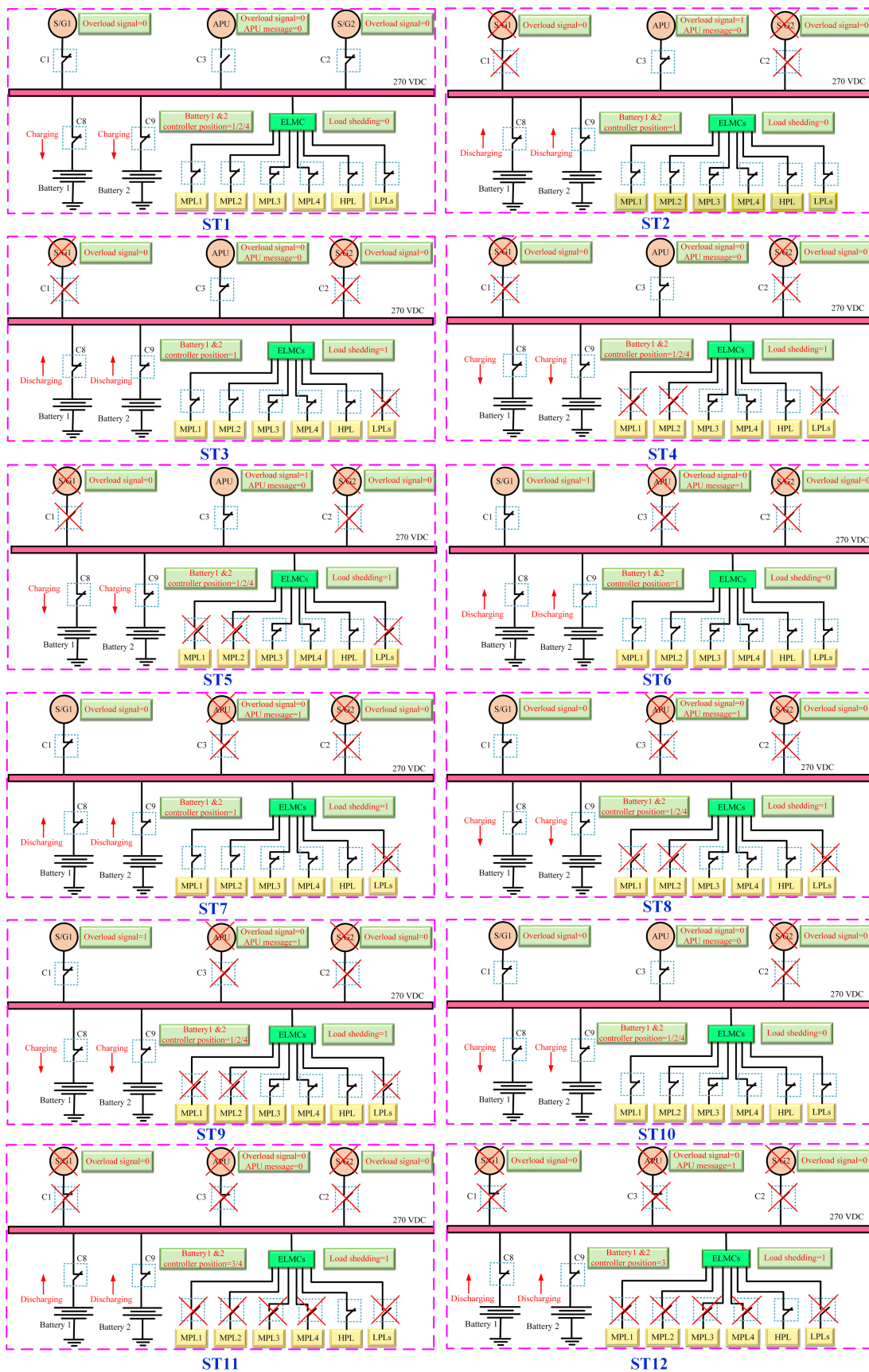


Fig. 4. States illustration on simplified EPS

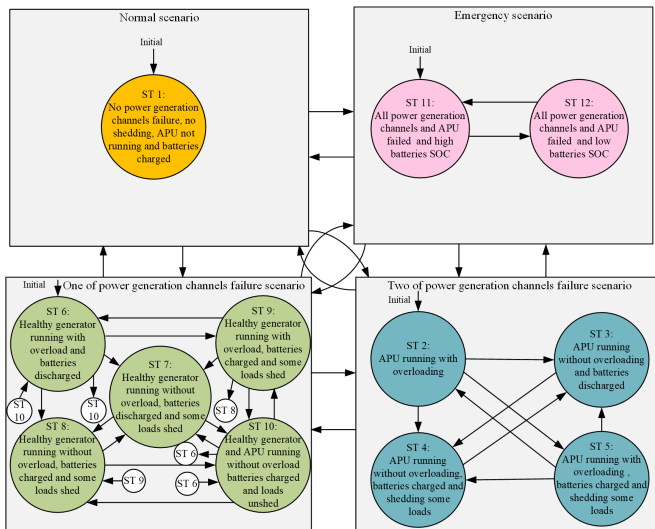


Fig. 5. Power distribution state diagram

within this main scenario as shown by the directions of the arrows, depending on the specified conditions. However, if the other generator fails while the APU continues to operate, the EM system will switch to ST2 and begin with the scenario “both main generators fail while APU running”. The internal transition is carried out in the same manner as described earlier. While in this scenario and an APU fails, it will switch to the emergency scenario, and if one of the main generators fault has been cleared, it will move to the scenario “one of the main generators fail”.

F. State Transition

The conditions of transition between different states (summarised in Table II) are defined by the status of generators, overload, and *SoC* of batteries. Table III shows the status of the generator during different scenarios e.g. if SG1 and SG2 status is normal, the EPS operates in ST1. Table IV indicates the status of switches, load shedding signal, overload signal, APU message, and a reference voltage and power values sent to the controllers. The value “0” indicates the switch is off (open) and the value “1” refers to the switch is on (closed). The battery controller switch has 4 control positions (1 to 4); DC power, battery terminal voltage, DC bus voltage, and halt, respectively [22]. The charging power P_{chn} is chosen here to be 30 kW for each battery pack and the maximum discharge power P_{dischn} to be 75 kW. The reference voltage for the battery cascaded voltage controller V_{dcn} is set 270 V. In conclusion, the EPS states for the proposed EM strategy, and the implementation of the proposed EM method utilizing the FSM technique have been presented. The criteria for transitions between the distinct states were also described, based on the status of EPS variables such as generator status. The effectiveness of the proposed EM strategy will be verified in the following section.

IV. SIMULATION RESULTS

This section applies the EM strategy proposed in Section II. The optimal droop gains design which was developed

in [23] is used here as the power-sharing method between sources. This proposed power-sharing approach guarantees that the system losses under different EPS reconfigurations are minimized. The multifunction battery controller introduced in [22] is used to reschedule the charging and discharging of the batteries. The battery controller switch has four positions namely; (1) DC power control, (2) battery voltage control, (3) DC bus voltage control, and (4) battery halt. The EPS shown in Fig. 1 is implemented using Matlab/Simulink environment for verification study. The two main generators, the APU, and their corresponding converters are modelled as current sources as in this paper it is required to control the output current [10]. The average model of the battery converter is assumed and the loads are modelled as constant power loads. The batteries are used to start the APU and the remaining *SoC* of the battery pack is assumed to be 70 % after starting the APU. Different scenarios are considered i.e. (A) normal scenario (B) one of power generation channels failure scenario (C) both of power generation channels failure scenario. The droop gains design for EPS with converters of different power ratings and different efficiencies is considered. The EPS parameters and ratings of converters are shown in Table V. The total system losses using optimal droop gain design [23] and conventional droop gain design methods are compared [24]. The optimal and conventional droop gains can be calculated as in (7) and (8), respectively.

$$R_{di-opt} = R_{esi} \quad (7)$$

where R_{di-opt} is optimal droop gain of the i^{th} converter and R_{esi} is the equivalent series resistance representing the copper losses of the converter i [23].

$$R_{di} = \frac{\Delta V_{max}}{I_{cimax}} \quad (8)$$

where ΔV_{max} and I_{cimax} are the maximum allowable voltage drop and the maximum output current of converter i , respectively.

A. Normal Scenario

In this part of the study, a normal flight operation is investigated with scenario as given in Table VI. Fig. 6 and Fig. 7 show the simulation results for this scenario. In the beginning, the EMC sent the signals to the ELMCs to connect the ground loads during movement on the ground, e.g. taxiing, landing, towing, etc, therefore, after starting the two main generators, they share the loads equally. If the *SoC* of the batteries is below the 95%, then, the batteries are charged with constant current until SoC_{max1} , which is assumed to be 80% in this study. The batteries continue charging up to SoC_{max} (95%) with constant voltage. The charging current of the battery according to the manufacturer specifications, is limited by 20 A and the voltage is 148 V as shown in Fig. 6 (g). After *SoC* reaches to 95 % the EMC stops the the charging of the batteries. During the flight, the EMC sends signals to the ELMCs to manage the loads in each flight phase according to the corresponding time as shown in Fig. 7. It should be noted that the DC bus voltage is kept within the limits 250-280 V according to MIL-STD-704F [25] as evidenced Fig. 6 (a).

TABLE II
STATES TRANSITION FOR DIFFERENT SCENARIOS

| Transition from | Condition | Transition to |
|--|---|---------------|
| Normal scenario (ST1) | Failure of two main generator | ST2 |
| Normal scenario (ST1) | Failure of one main generator | ST6 |
| Normal scenario (ST1) | Failure of two main generator and APU | ST11 |
| One of power generation channels failure scenario (any states) | Fault of power generation channels is cleared | ST1 |
| One of power generation channels failure scenario (any states) | Other power generation channels are failed APU is started | ST2 |
| One of power generation channels failure scenario (any states) | Other power generation channels are failed APU is failed/not started | ST11 |
| Two of power generation channels failure scenario (any states) | Fault of power generation channels is cleared | ST1 |
| Two of power generation channels failure scenario (any states) | One of power generation channels fault is cleared | ST6 |
| Two of power generation channels failure scenario (any states) | APU is failed/not started | ST11 |
| Emergency scenario (any states) | If both of power generation channels fault is cleared | ST1 |
| Emergency scenario (any states) | If any one of power generation channels fault is cleared | ST6 |
| Emergency scenario (any states) | If both of power generation channels failed and APU running | ST2 |
| ST2, ST5 | The overload of APU is reached $SoC_{1,2} > SoC_{min}$ | ST3 |
| ST2, ST5, ST3 | The overload of APU is reached $SoC_{1,2} < SoC_{min}$ | ST4 |
| ST2 | The overload of APU is not reached $SoC_{1,2} < SoC_{min}$ | ST5 |
| ST4 | The overload of APU is reached $SoC_{1,2} > SoC_{max}$ | ST3 |
| ST5 | The overload of APU is not reached $SoC_{1,2} > SoC_{max}$ | ST2 |
| ST6, ST9, and ST10 | The overload of healthy generator is reached $SoC_{1,2} > SoC_{min}$ APU is not started | state 7 |
| ST8 | The overload of healthy generator is reached $SoC_{1,2} > SoC_{max}$ APU is not started | ST7 |
| ST6, ST7, ST9, and ST10 | The overload of healthy generator is reached $SoC_{1,2} < SoC_{min}$ APU is not started | ST8 |
| ST6, ST10 | The overload of healthy generator is not reached $SoC_{1,2} > SoC_{min}$ | ST9 |
| ST6, ST7, ST8, and ST9 | APU is started | ST10 |
| ST10 | APU is failed The overload of healthy generator is not reached $SoC_{1,2} > SoC_{min}$ | ST6 |
| ST9 | APU is not running Overload of healthy generator is not reached $SoC_{1,2} > SoC_{max}$ | ST6 |
| ST11 | All power generation channels are failed $SoC_{1,2} > SoC_{min}$ | ST12 |
| ST12 | All power generation channels are failed $SoC_{1,2} < SoC_{min}$ | ST11 |

TABLE III
STATUS OF GENERATORS, BATTERIES SoC AND OVERLOADING TIME DURING DIFFERENT SCENARIOS

| Scenario | Normal | Two of Power Generation channels failure | | | | One of power generation channels failure | | | | Emergency | | |
|-----------------|-------------|--|--------------|--------------|--------------|--|--------------|--------------|--------------|-------------|--------------|--------------|
| | | ST1 | ST2 | ST3 | ST4 | ST 5 | ST6 | ST7 | ST 8 | ST9 | ST10 | ST11 |
| G1 status | N | F | F | F | F | F | N/F | N/F | N/F | N/F | F | F |
| G2 status | N | F | F | F | F | F | N/F | N/F | N/F | N/F | F | F |
| APU status | NR | N | N | N | N | NR/F | NR/F | NR/F | NR/F | N | F | F |
| State of charge | Do not care | $>SoC_{max}$ | $>SoC_{min}$ | $<SoC_{min}$ | $<SoC_{min}$ | $>SoC_{min}$ | $>SoC_{min}$ | $<SoC_{min}$ | $<SoC_{min}$ | Do not care | $<SoC_{min}$ | $>SoC_{min}$ |
| Overload period | Non | Not reached | Reached | Reached | Not reached | Not reached | Reached | Reached | Not reached | Non | Non | Non |

N= Normal, F= Failure, NR= Not running

Comparison between optimal [23] and conventional droop gains design for the power-sharing between sources is investigated. This comparison considers the total system losses including converters, transmission lines losses and battery losses (inductor and internal resistance) during the normal flight. It is clear from Fig. 8 that the optimal droop gains design provides reduced losses in comparison to the conventional design, the total EPS losses under conventional droop control are 107 kW while under the optimal droop one they are 94

kW, i.e. they are reduced by 13 kW (or 11.3%) during the flight.

B. One of power generation channel failure case

The failure of the main generator 1 simulated covering STs 6, 7, 8, and 10. The simulation results are shown in Fig. 9 and Fig. 10. The flight started normally, as the both main generators supplied the loads together, in addition to charging the batteries until these reach the maximum SoC value (95%).

TABLE IV
SYSTEM SWITCHES AND VARIABLES SETTINGS

| Scenario | Normal | Two of Power Generation channels failure | | | | | One of power generation channels failure | | | | | Emergency | |
|-----------------------------|-------------|--|--------------|-----------|-----------|--------------|--|-----------|-----------|-----------|------|-----------|--|
| State | ST1 | ST2 | ST3 | ST4 | ST5 | ST6 | ST7 | ST8 | ST9 | ST10 | ST11 | ST12 | |
| SSPC1 switch | 1 | 0 | 0 | 0 | 0 | 0/1 | 0/1 | 0/1 | 0/1 | 0/1 | 0 | 0 | |
| SSPC2 switch | 1 | 0 | 0 | 0 | 0 | 0/1 | 0/1 | 0/1 | 0/1 | 0/1 | 0 | 0 | |
| SSPC3 switch | 0 | 1 | 1 | 1 | 1 | 0 | 0 | 0 | 0 | 1 | 0 | 0 | |
| SSPC8 switch | 0/1 | 1 | 1 | 1 | 1 | 1 | 1 | 1 | 1 | 1 | 1 | 1 | |
| SSPC9 switch | 0/1 | 1 | 1 | 1 | 1 | 1 | 1 | 1 | 1 | 1 | 1 | 1 | |
| Load shedding | 0 | 1 | 1 | 1 | 1 | 0 | 1 | 1 | 1 | 0 | 1 | 1 | |
| Overload signal | 0 | 1 | 0 | 0 | 1 | 1 | 0 | 0 | 1 | 0 | 0 | 0 | |
| APU message | 0 | 0 | 0 | 0 | 0 | 1 | 1 | 1 | 1 | 0 | 1 | 1 | |
| Battery controller switch | 1/2/4 | 1 | 1 | 1/2/4 | 1/2/4 | 1 | 1 | 1/2/4 | 1/2/4 | 1/2/4 | 3/4 | 3 | |
| Battery 1 reference power | $P_{chn}/0$ | P_{dischn} | P_{dischn} | P_{chn} | P_{chn} | P_{dischn} | P_{dischn} | P_{chn} | P_{chn} | P_{chn} | 0 | 0 | |
| Battery 2 reference power | $P_{chn}/0$ | P_{dischn} | P_{dischn} | P_{chn} | P_{chn} | P_{dischn} | P_{dischn} | P_{chn} | P_{chn} | P_{chn} | 0 | 0 | |
| Battery 1 reference voltage | V_{dcn} | | | | | | | | | | | | |
| Battery 2 reference voltage | V_{dcn} | | | | | | | | | | | | |

TABLE V
CONVERTERS, TRANSMISSION LINE DATA, AND OPTIMAL DROOP GAINS VALUES

| | Converter 1 | Converter 2 | Converter 3 | Battery 1 | Battery 2 |
|---------------------------------------|-------------|-------------|-------------|-----------|-----------|
| Rating | 300 (kW) | 300 (kW) | 300 (kW) | 75 (kWh) | 75 (kWh) |
| DC voltage (V) | 270 | | | | |
| Rated current (A) | 1112 | 1112 | 1112 | 278 | 278 |
| Efficiency (%) | 98 | 95 | 97 | 97 | 95 |
| Droop gain Ω | 0.01214 | 0.01214 | 0.01214 | 0.0486 | 0.0486 |
| Converter resistance (Ω) | 0.0042 | 0.0109 | 0.0064 | 0.0256 | 0.0435 |
| No load losses (W) | 918.38 | 2368.4 | 1391.4 | 347.9 | 592.1 |
| Transmission resistances (Ω) | 0.0012 | 0.0012 | 0.0012 | 0.0049 | 0.0049 |

TABLE VI
TIME AND NUMBERS OF FLIGHT PHASES

| Flight phase | Ground | Take off | Climb | Cruise | Descending | Loiter | Landing |
|-----------------------|--------|----------|-------|--------|------------|--------|---------|
| Flight phase number | 1 | 2 | 3 | 4 | 5 | 6 | 7 |
| Time | t_1 | t_2 | t_3 | t_4 | t_5 | t_6 | t_7 |
| Flight phase time (s) | 600 | 300 | 600 | 3600 | 300 | 300 | 600 |

After reaching the maximum value, the charging will stop. At $t=1600s$ during the cruise, a fault in the main generator occurs. The EM responds to this fault by going to ST6 directly. In this state, a signal is sent to the APU generator to prepare to start and to share the loads, and the remaining healthy main generator is allowed to overload by 10%. After 50s, the APU generator is ready to share the loads with the main generator. The overload of the main generator is cleared, and the batteries are charging until they reach the maximum SoC values; this covers ST10. At $t=1900s$ a fault occurs in the APU generator, and in this case, the healthy main generator is allowed to overload again and the batteries are allowed to provide 70 kW of power (ST6). As mentioned above, the healthy generator is allowed to overload for a period of 300s (5mins), at $t=2200s$ the overload period expires consequently, the batteries need to supply the required power, gradually discharging until SoC drop to its the minimum SoC value (ST7). At $t=2665s$, the SoC reaches the minimum values (28%). Therefore, they will start charging after shedding LPLs and part1 and part two of MPLs (ST8). At $t=3920s$ the SoC reach their maximum values and the EMC sends the signal to discharge the batteries (ST7). Such a cycle of charging/discharging will continue until the end of the flight. It is clear from Fig. 9 (a) the main DC bus and local DC buses voltages are kept within the acceptable limits. Fig. 11 shows the total system losses during the whole flight using conventional and optimal droop gains [23] methods, and

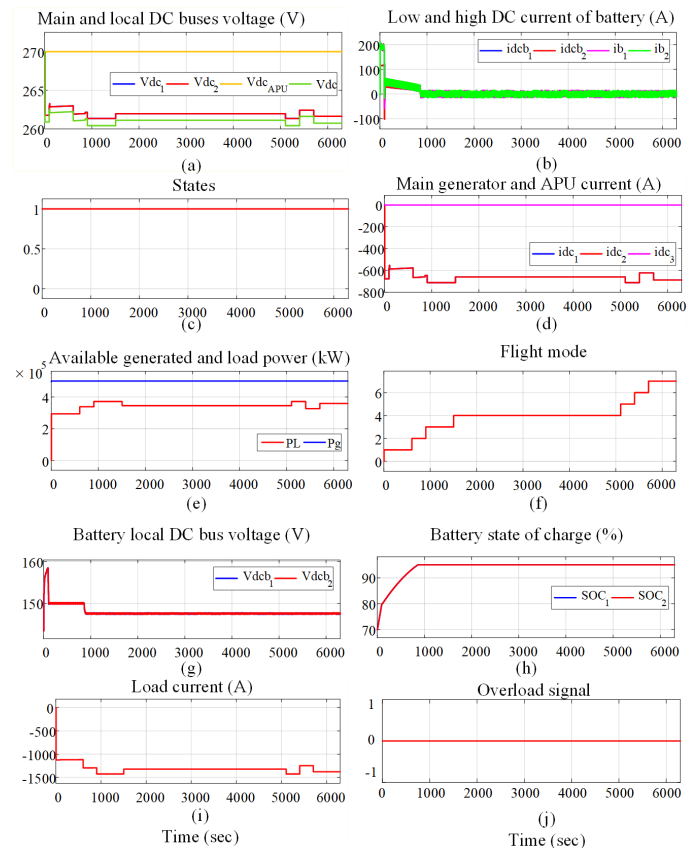


Fig. 6. Simulation results under normal flight scenario

it is clear from this figure that the losses in the case of the conventional method are 218 kW against 209 kW in the case of the optimal design, a reduction of 9 kW (4%) for the optimal design. Accordingly, the method of optimal droop gain design gives fewer losses compare to the traditional method.

C. Loss of both main power generation scenario

The performance of the EPS under a failure of both main generators using conventional and optimal droop gains was evaluated as well. This scenario runs through STs2, 3, 4, 5, 11, and 12. Fig. 12 and Fig. 13 show the simulation results. Initially, the aircraft flies normally (ST1) and at $t=1600s$

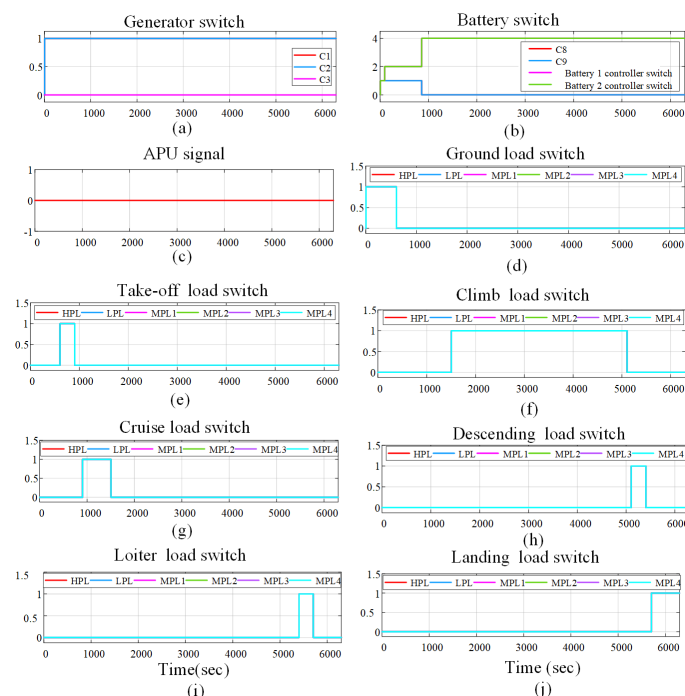


Fig. 7. Switching states, reference battery voltage, APU signal and overload signal under normal flight scenario

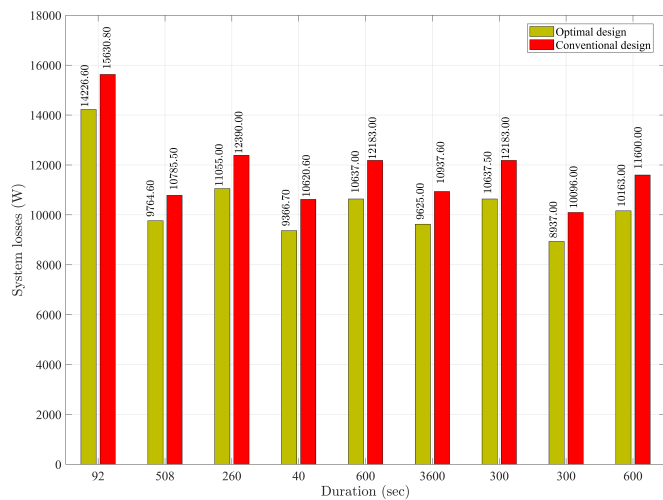


Fig. 8. Total System losses under normal scenario

during the cruise, the aircraft loses both main power generators simultaneously. According to the EM strategy the EMC commands to start APU. Until the APU started the batteries are giving supply to the HPLs, as the only option for the pilot is to doing hard landing (ST12). The batteries' voltage controller is activated replacing the batteries power control since it is critical to maintain the DC bus voltage at correct level. After (100s from sending the command from the EMC), the APU is ready to supply the loads with overloading allowed, along with the batteries and therefore all the loads are unshaded (ST2). The total load is 345 kW and the APU delivers 275 kW,

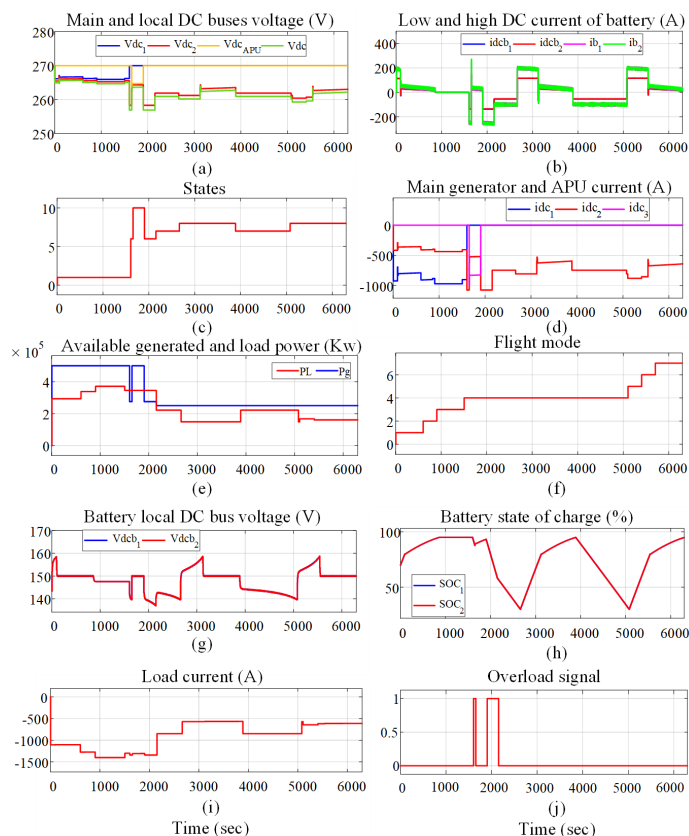


Fig. 9. Simulation results under one of power generation channel failure scenario

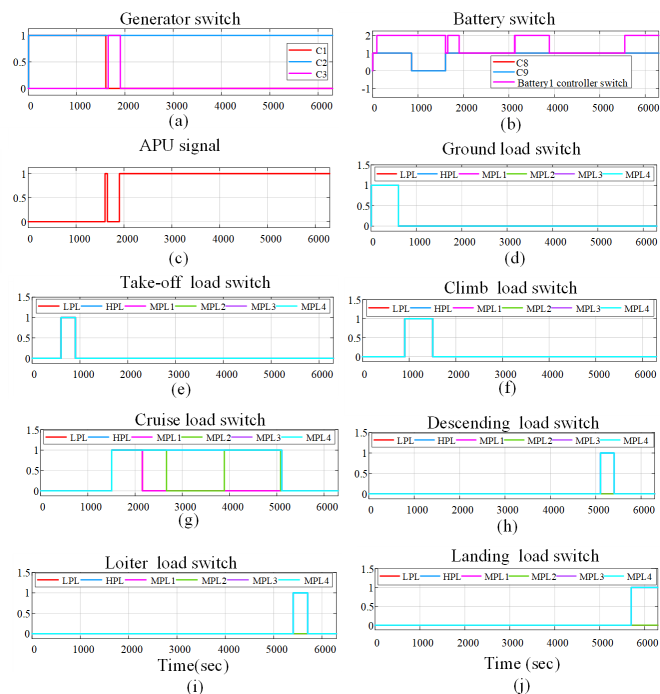


Fig. 10. Switching states, reference battery voltage, APU signal and overload signal under one of power generation channels failure scenario

therefore the batteries supply the difference which is 70 kW. At $t=1800s$ the APU also fails, so the EMC sent asks the ELMC

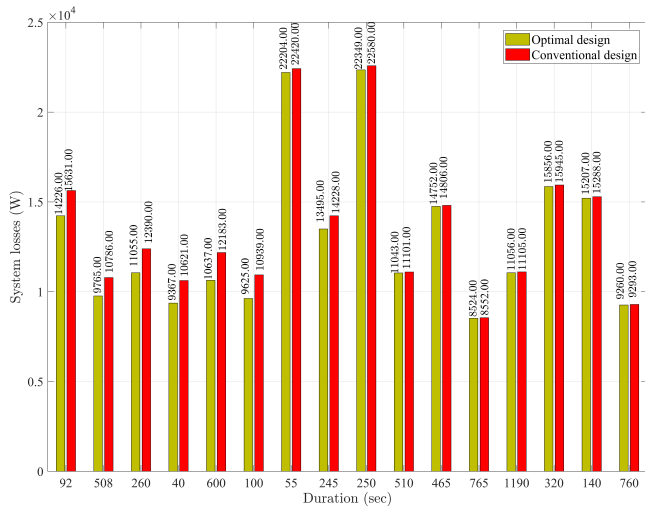


Fig. 11. Total System losses under one of power generation channel failure scenario

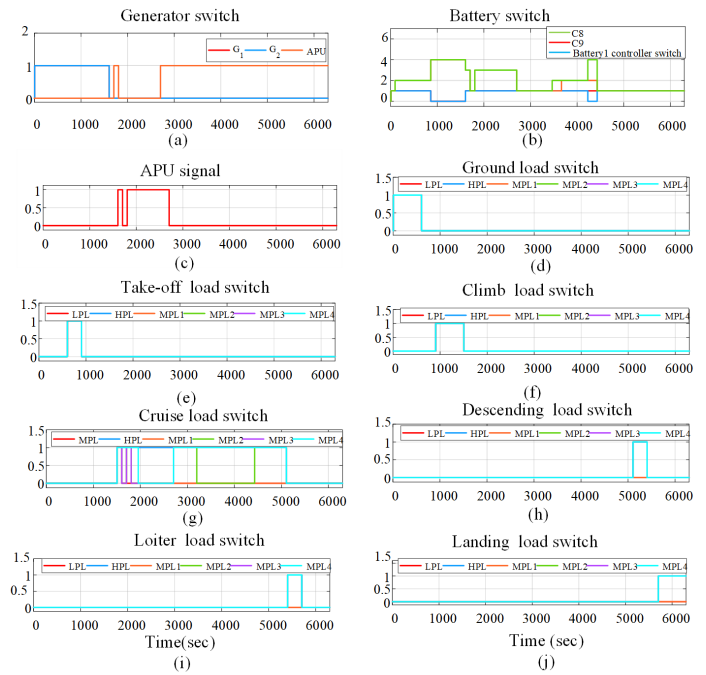


Fig. 13. Switching states, reference battery voltage, APU signal and overload signal under both of power generation channels failure scenario

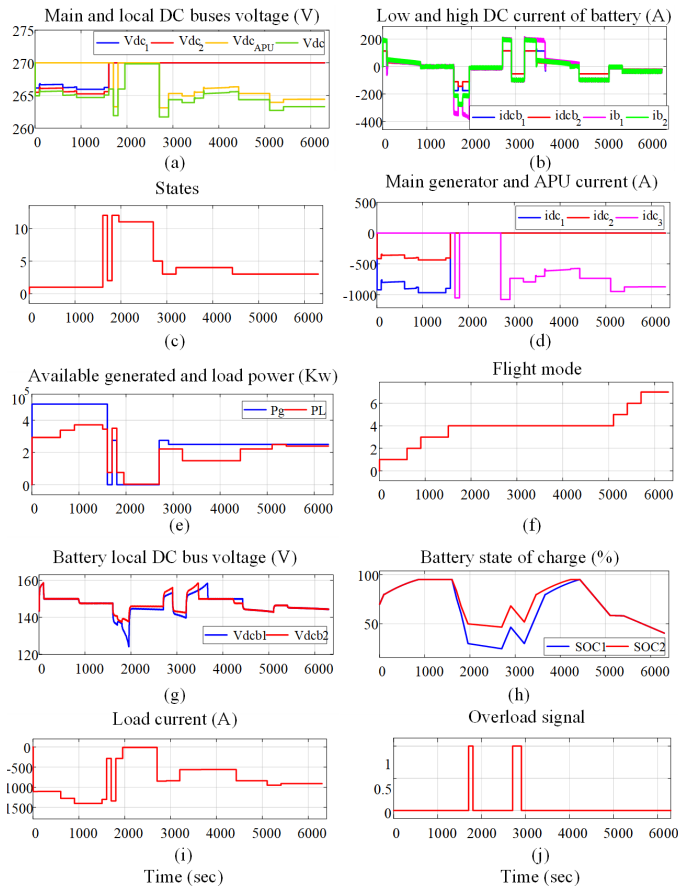


Fig. 12. Simulation results under both of power generation channel failure scenario

to shed all loads apart from only part 4 of MPL and HPLs (ST12). When the *SoC* reaches its minimum value the part 4 of MPLs are also shed and only the HPLs are powered until the aircraft land safely (ST11). It should be noted that the two battery systems are discharged with different currents because

they have different optimal droop control gains as shown in Fig. 12 (h). At $t=2700$ s the APU is back to work with overload capability, so the available power is 275 kW. Therefore, the LPLs and part 1 of MPLs are unshed and the batteries are charged (ST5). The overload period is ended at 2900s, and the EMC goes into ST3, at which point the batteries are supplying the deficit in power between the APU and the loads. Moreover, the LPLs, part 1 of MPLs are shed as shown in Fig. 13 (c). When the batteries are fully discharged ($SoC < 28\%$), the EM moves to ST4, in which the LPLs, part 1 and 2 of medium priority loads are shed to allow the batteries to charge. At $t=4430$ s the *SoC* of batteries are reaches the maximum value, therefore the system backs into ST3. When the batteries *SoC* drops below their minimum values the EMC sheds the LPLs and part one and part two of MPLs, and batteries start to charge again (ST4). It should be noted that the load current changes according to loads of each flight phase as shown in Fig. 12 (i). It is clear from the results that the DC bus and local DC buses voltages are kept within the limits during the considered emergency case. The total EPS losses using the conventional and the optimal droop gains design are calculated during each flight phase as shown in Fig. 14. These were 202 kW for the conventional method but only 195 kW for the optimal droop gain design method [23]. This leads to a 7 kW (3.4%) reduction in losses in the studied scenario. It should be noted that the losses in some operation modes i.e. ST3, ST4, and ST11 using the optimal droop gains method are higher than the conventional method. This is because the batteries are charged/discharged with different power and due to using different droop gains. The batteries are charged with constant power/voltage but they have different *SoC*, and this leads to the time of charging for batteries pack 1 being longer than

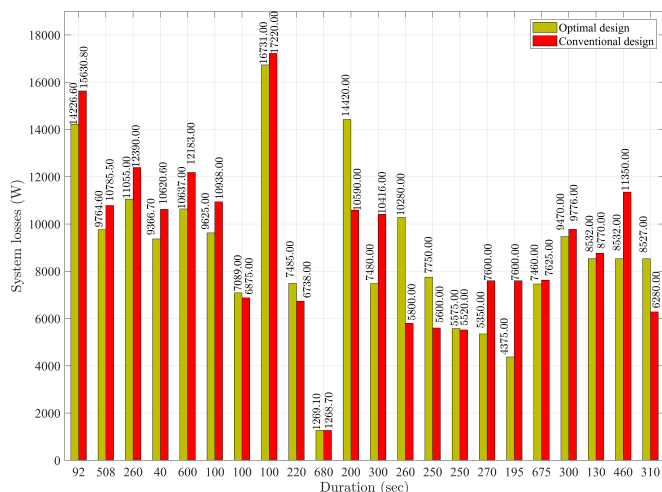


Fig. 14. Total System losses under both of power generation channel failure scenario

pack 2 in the considered case. Moreover, the losses will be slightly higher than the conventional method as the battery packs are fully charged at the same time. However, in general, the total system losses when optimal droop gains are applied are smaller than with the conventional method if the whole flight is considered.

V. HIL VALIDATION

In this section, the model which used in Matlab/Simulink is simulated on the Typhoon HIL 604 real-time power electronics emulator to evaluate the performance of the proposed EM control strategy. The setup of the HIL experiment is as shown in Fig. 15. The PMSM (operating in generation mode), the battery energy storage systems and three-phase inverters are modelled in the Typhoon device via the Typhoon software schematic editor. A Texas Instrument (TI) digital signal processor (DSP) (i.e. F2879D control card) is used to implement the energy management study and then send the control signals to the system components. The control card and the developed system plant in the typhoon software communicate via the interface board as shown in Fig. 15. Fig. 16 shows the results when the system moves from normal scenario (ST1) to failure of one of main generators scenario (ST6). It can be seen that the results are identical to those presented in Fig. 9 and Fig. 10.

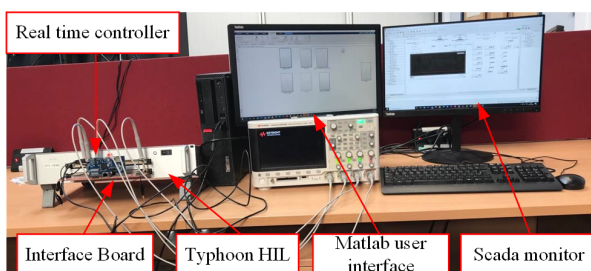


Fig. 15. HIL setup

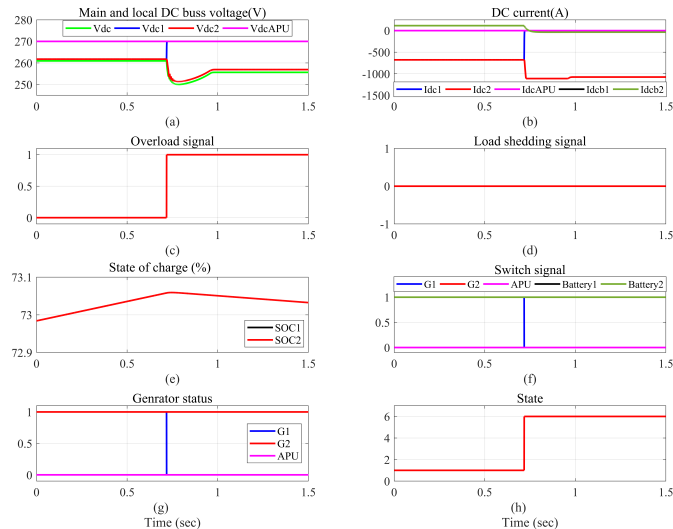


Fig. 16. HIL results for transition from ST1 to ST6

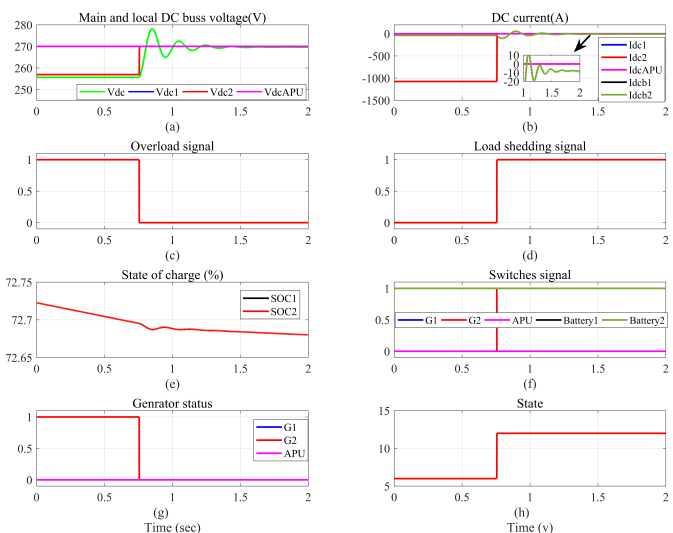


Fig. 17. HIL results for transition from ST6 to ST12

Regarding the system losses, it was found the reduction in losses equal 1418 W (9.4%) in ST1 and 155 W (1%) in ST6 when the optimal droop gain is employed. Fig. 17 shows the results when the other main generator is failed (ST12). In this case the batteries supply the HPLs and MPL1 until the SoC drops below the minimum value. It can be seen from Fig. 17, the DC bus voltage is kept around the nominal value 270 V by means of DC bus voltage battery controller. The system losses were nearly equal when the conventional and optimal droop gains are utilised and they are equal 1269 W. The Typhoon HIL simulation results show that the proposed EM control strategy can effectively supply the HPLs and reduce system losses under different scenarios in real time.

VI. CONCLUSION

In this paper, a proposed energy management strategy to minimize the total system losses and taking into account the thermal capability of the power generation sources, batteries schedules, and variable load priority for the representative EPS for future MEA is presented. The control logic of the proposed strategy is implemented using FSM. Moreover, it is tested and verified using different operating scenarios for complete flight i.e. normal, loss of one of power generation channels, and loss of two of power generation channels using Matlab/Simulink and Typhoon HIL platform. The simulation results show that the controller activates the correct state to always provide safety-critical loads for all fault conditions. Furthermore, it confirmed that the proposed method reduced the total system losses in all studied cases compared to the conventional method. The proposed method keeps the main DC bus and local DC buses voltage within standard limits. Further, the example aircraft can fly safely with one generator during the complete trip using the proposed EM strategy.

ACKNOWLEDGMENTS

This work was supported by the Egyptian Government ministry of higher education (cultural affairs and missions sector) and the British Council through Newton-Mosharafa fund. The authors also gratefully acknowledge support from the ESTEEM project which received funding from the Clean Sky 2 Joint Undertaking under the European Union's Horizon 2020 research and innovation programme under grant agreement No 755485.

REFERENCES

- [1] V. Madonna, P. Giangrande, and M. Galea, "Electrical power generation in aircraft: Review, challenges, and opportunities," *IEEE Transactions on Transportation Electrification*, vol. 4, no. 3, pp. 646–659, 2018.
- [2] B. Sarlioglu and C. T. Morris, "More electric aircraft: Review, challenges, and opportunities for commercial transport aircraft," *IEEE Transactions on Transportation Electrification*, vol. 1, no. 1, pp. 54–64, 2015.
- [3] A. S. Ian Moir, *Aircraft Systems: Mechanical, electrical and avoionics subsystems integration*. Willey, 2008.
- [4] K. Ni, Y. Liu, Z. Mei, T. Wu, Y. Hu, H. Wen, and Y. Wang, "Electrical and electronic technologies in more-electric aircraft: A review," *IEEE Access*, vol. 7, pp. 76 145–76 166, 2019.
- [5] K. Emadi and M. Ehsani, "Aircraft power systems: Technology, state of the art, and future trends," *IEEE Aerospace and Electronic Systems Magazine*, vol. 15, no. 1, pp. 28–32, 2000.
- [6] P. W. Wheeler, J. C. Clare, A. Trentin, and S. Bozhko, "An overview of the more electrical aircraft," *Proceedings of the Institution of Mechanical Engineers, Part G: Journal of Aerospace Engineering*, vol. 227, no. 4, pp. 578–585, 2013.
- [7] A. Y. Arabul, E. Kurt, F. K. Arabul, İbrahim Senol, M. Schrötter, R. Bréda, and D. Megyesi, "Perspectives and development of electrical systems in more electric aircraft," *International Journal of Aerospace Engineering*, 2021.
- [8] J. Chen, C. Wang, and J. Chen, "Investigation on the selection of electric power system architecture for future more electric aircraft," *IEEE Transactions on Transportation Electrification*, vol. 4, no. 2, pp. 563–576, 2018.
- [9] J. Brombach, A. Lücken, B. Nya, M. Johannsen, and D. Schulz, "Comparison of different electrical hvdc-architectures for aircraft application," in *2012 Electrical Systems for Aircraft, Railway and Ship Propulsion*, 2012, pp. 1–6.
- [10] F. Gao, "Decentralised control and stability analysis of a multi-generator based electrical power system for more electric aircraft," PhD thesis, University of Nottingham, August 2016.
- [11] D. Izquierdo, R. Azcona, F. J. L. d. Cerro, C. Fernández, and B. Delicado, "Electrical power distribution system (hv270dc), for application in more electric aircraft," in *2010 Twenty-Fifth Annual IEEE Applied Power Electronics Conference and Exposition (APEC)*, 2010, pp. 1300–1305.
- [12] J. CHEN, "Study of 270vdc system application," Master's thesis, School of Engineering, Aircraft Design Programme, Cranfield University, 2009–2010.
- [13] D. Schlabe and J. Lienig, "Energy management of aircraft electrical systems - state of the art and further directions," in *2012 Electrical Systems for Aircraft, Railway and Ship Propulsion*, 2012, pp. 1–6.
- [14] P. Saenger, K. Deschinkel, N. Devillers, and M. Pera, "An optimal sizing of electrical energy storage system for an accurate energy management in an aircraft," in *2015 IEEE Vehicle Power and Propulsion Conference (VPPC)*, 2015, pp. 1–6.
- [15] C. Spagnolo, S. Sumsurooah, C. I. Hill, and S. Bozhko, "Smart controller design for safety operation of the me electrical distribution system," in *IECON 2018 - 44th Annual Conference of the IEEE Industrial Electronics Society*, 2018, pp. 5778–5785.
- [16] X. Giraud, H. Piquet, M. Budinger, X. Roboam, M. Sartor, and S. Vial, "Knowledge-based system for aircraft electrical power system reconfiguration," in *2012 Electrical Systems for Aircraft, Railway and Ship Propulsion*, 2012, pp. 1–6.
- [17] B. Tang, S. Yang, L. Wang, and H. Zhang, "Power priority algorithm in application to aircraft distribution network reconfiguration," in *2016 International Conference on Electrical Systems for Aircraft, Railway, Ship Propulsion and Road Vehicles International Transportation Electrification Conference (ESARS-ITEC)*, 2016, pp. 1–5.
- [18] Y. Yang and Z. Gao, "Power management problem for civil aircraft under more electric environment," *International Journal of Aerospace Engineering Journal*, vol. 2020, 2020.

- [19] A. Barzegar, R. Su, C. Wen, L. Rajabpour, Y. Zhang, A. Gupta, C. Gajanayake, and M. Y. Lee, "Intelligent power allocation and load management of more electric aircraft," in *2015 IEEE 11th International Conference on Power Electronics and Drive Systems*, 2015, pp. 533–538.
- [20] Xuesen Lin, "Multi-behaviors finite state machine," in *2009 IEEE Youth Conference on Information, Computing and Telecommunication*, 2009, pp. 201–203.
- [21] P. Nuzzo, H. Xu, N. Ozay, J. B. Finn, A. L. Sangiovanni-Vincentelli, R. M. Murray, A. Donz , and S. A. Seshia, "A contract-based methodology for aircraft electric power system design," *IEEE Access*, vol. 2, pp. 1–25, 2014.
- [22] M. A. A. Mohamed, S. Yeoh, J. Atkin, M. Khalaf, and S. Bozhko, "Analysis and design of battery controller for more electric aircraft application," in *2021 IEEE International Power and Renewable Energy Conference (IPRECON)*, 2021, pp. 1–6.
- [23] M. A. Mohamed, M. Rashed, X. Lang, J. Atkin, S. Yeoh, and S. Bozhko, "Droop control design to minimize losses in dc microgrid for more electric aircraft," *Electric Power Systems Research*, vol. 199, p. 107452, 2021.
- [24] X. Lu, J. M. Guerrero, K. Sun, and J. C. Vasquez, "An Improved Droop Control Method for DC Microgrids Based on Low Bandwidth Communication With DC Bus Voltage Restoration and Enhanced Current Sharing Accuracy," *IEEE Transactions on Power Electronics*, vol. 29, no. 4, pp. 1800–1812, 2014.
- [25] *MIL-STD-704F Aircraft Electrical Power Characteristics*, Department of Defence Interface Standard, 2004.



Jason A. Atkin received the B.Sc. degree in mathematics with computing in 1992 and the Ph.D. degree in computer science in 2008 from the University of Nottingham, Nottingham, U.K. He is an Associate Professor with the Computational Optimisation and Learning (COL) Lab, School of Computer Science, University of Nottingham. He initially was a Software Engineer, Consultant, and Team Leader, before joining University of Nottingham in 2003. His research currently involves finding fast solution methods for real-world optimization, design and control problems, using exact, heuristic, and hybrid algorithms and/or automated code generation. He currently leads the air transportation modeling and optimization within COL, having been working in this area since 2003, and has algorithms running live at Heathrow airport.



Habibu Hussaini received the B.Eng. degree in electrical and computer engineering from the Federal University of Technology, Minna, Nigeria, in 2010, the M.Sc. degree in energy and sustainability with electrical power engineering from the University of Southampton, Southampton, U.K., in 2015. He is currently working toward the Ph.D. degree in electrical and electronics engineering with the University of Nottingham, Nottingham, U.K. His research interests include aircraft electrical power systems, artificial intelligence, power electronics and control.

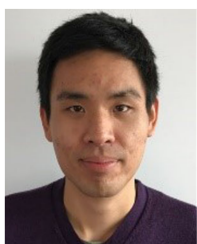


Serhiy Bozhko (Senior Member, IEEE) received the M.Sc. and Ph.D. degrees in electromechanical systems from the National Technical University of Ukraine, Kyiv City, Ukraine, in 1987 and 1994, respectively. Since 2000, he has been with the Power Electronics, Machines and Controls Research Group, University of Nottingham, Nottingham, U.K., where he is currently a Professor of Aircraft Electric Power Systems and the Director of the Institute for Aerospace Technology. He is leading several EU- and industry funded projects in the area of aircraft electric power systems, including power generation, distribution and conversion, power quality, control and stability issues, power management and optimization, as well as advanced modeling and simulations methods.



Mohamed A. A. Mohamed (Graduate Student Member, IEEE) received the B.Sc. (hons.) and M.Sc. (hons.) degrees in electrical engineering (power and electric machines) from Assiut University, Assiut, Egypt in 2010 and 2015, respectively. In 2022, he received the PhD degree in electrical engineering (Power Electronics, Machines and Control Group), Nottingham University, Nottingham, UK. Since then, he has been a Research Fellow with WMG, University of Warwick. His research interests include More-Electric Aircraft (MEA) applications,

Electrical Power System for MEAs including their architectures, Advanced modelling, Control and stability issues of MEA power system, Smart energy management in DC micro-grids, and battery management systems.



Seang Shen Yeoh received his MSc degree in power electronics (Distinction) and Ph.D degree in electrical engineering from the University of Nottingham, United Kingdom, in 2011 and 2016 respectively. Since then, he has been a research fellow in the same university under the Power Electronics, Machines, and Controls Research Group. His current research interests are in the area of aircraft power systems, namely modelling and stability studies of complex power systems, and new control strategies for high speed drive systems.